Supplement of Geosci. Model Dev., 17, 4401–4432, 2024
https://doi.org/10.5194/gmd-17-4401-2024-supplement

Geoscientific Model Development
Open Access
EGU

Supplement of

An improved and extended parameterization of the CO_2 15 μm cooling in the middle and upper atmosphere (CO2_cool_fort-1.0)

Manuel López-Puertas et al.

Correspondence to: Manuel López-Puertas (puertas@iaa.es)

This document serves as a supplement material for the main paper.

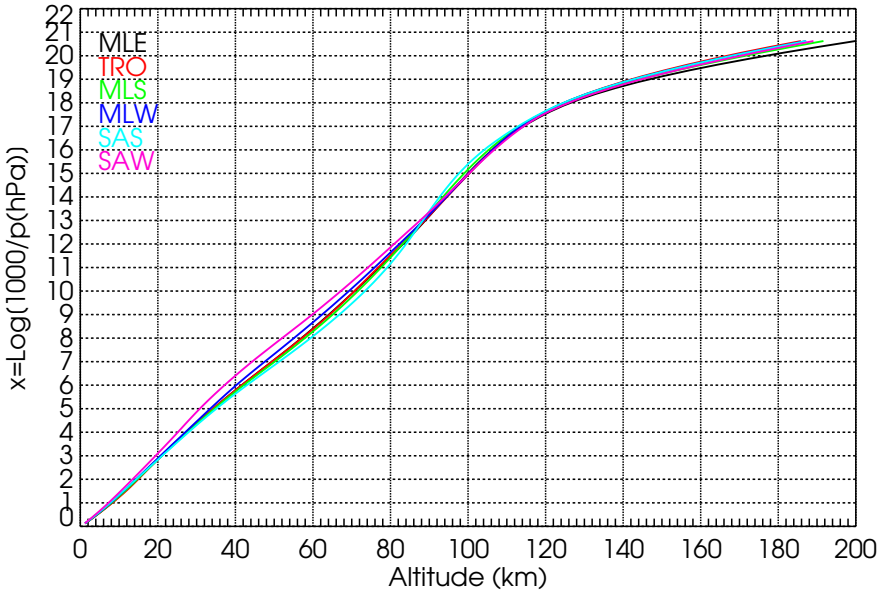

Figure S1. The relationship between pressure and geometrical altitude for the reference temperature profiles.

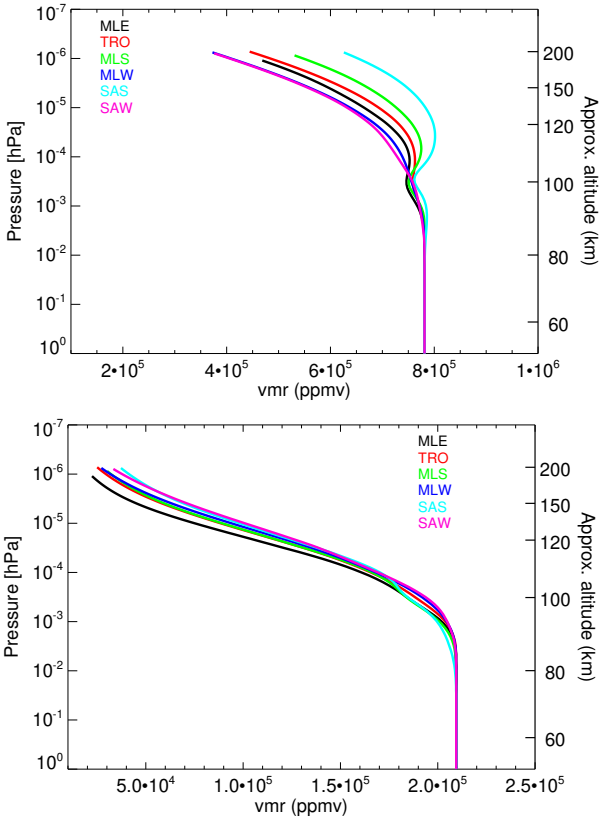

Figure S2. N_2 (top) and O_2 (bottom) volume mixing ratio profiles for the respective atmospheric conditions used in the references calculations.

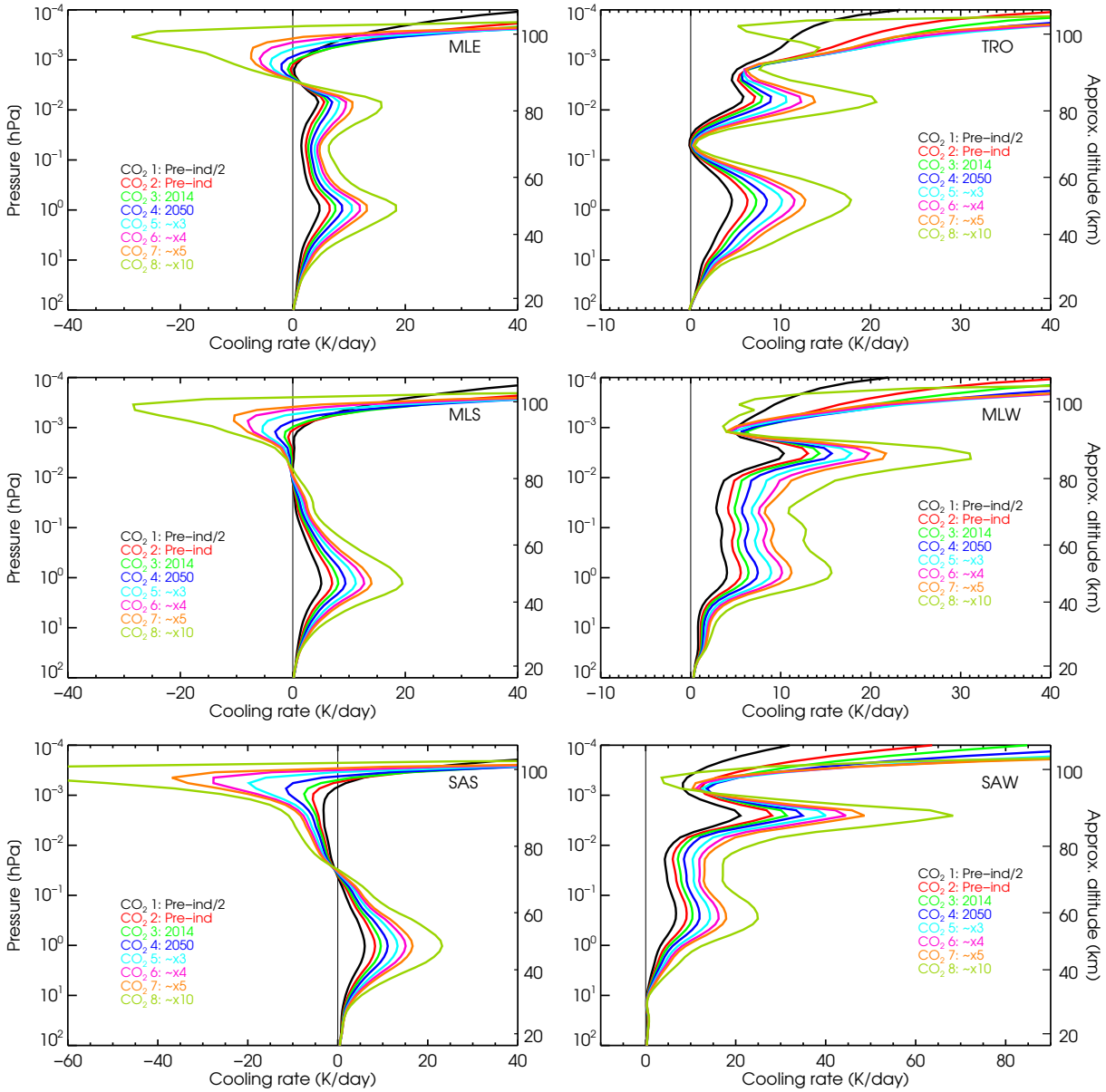

Figure S3. The LTE cooling rates for the reference atmospheres shown up to the lower thermosphere. Note the different x-scales. The cooling rates extended up to the thermosphere are shown in Fig. S4 below.

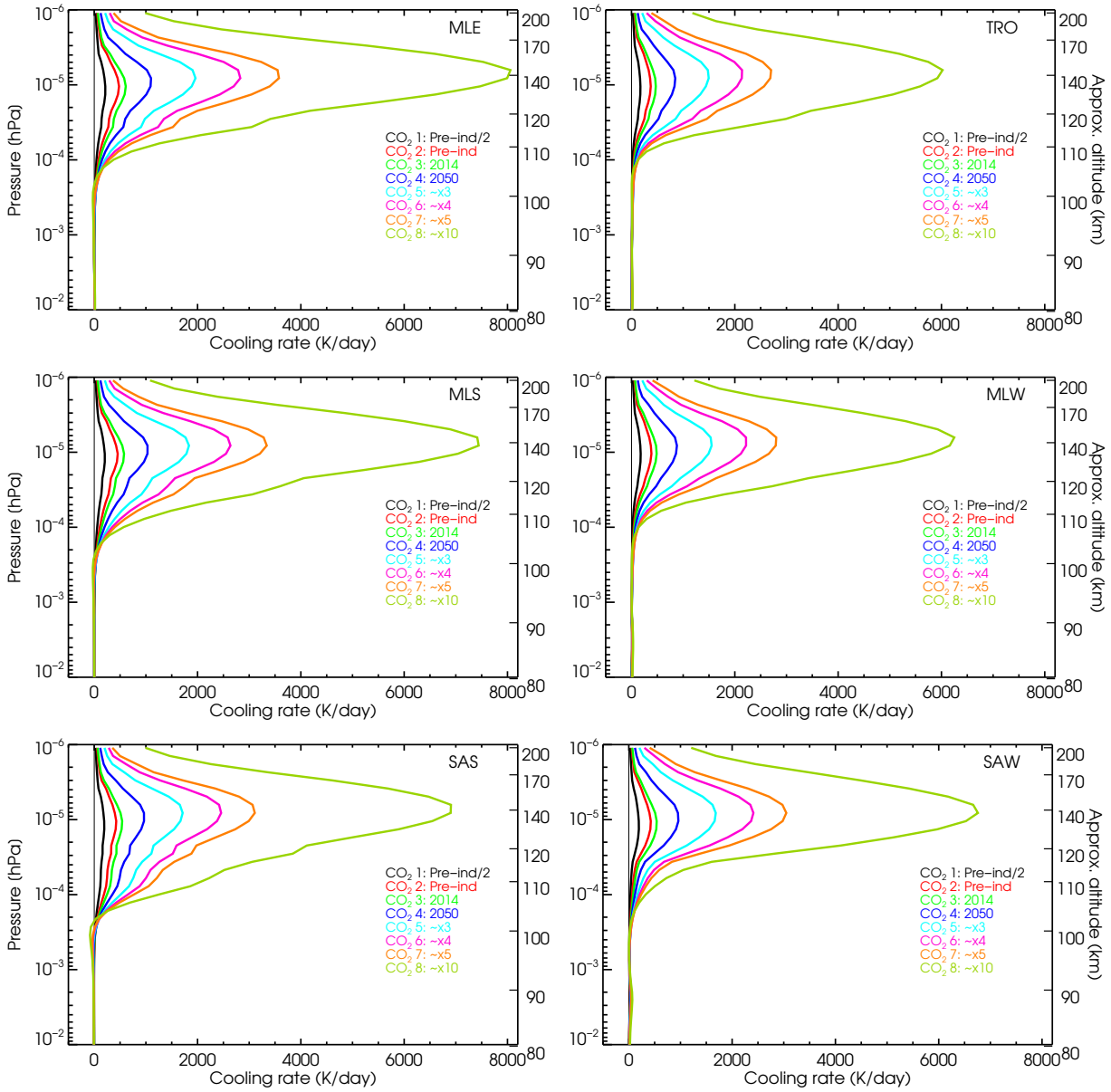

Figure S4. The LTE cooling rates for the reference atmospheres. As in Fig. S3 but covering the thermosphere.

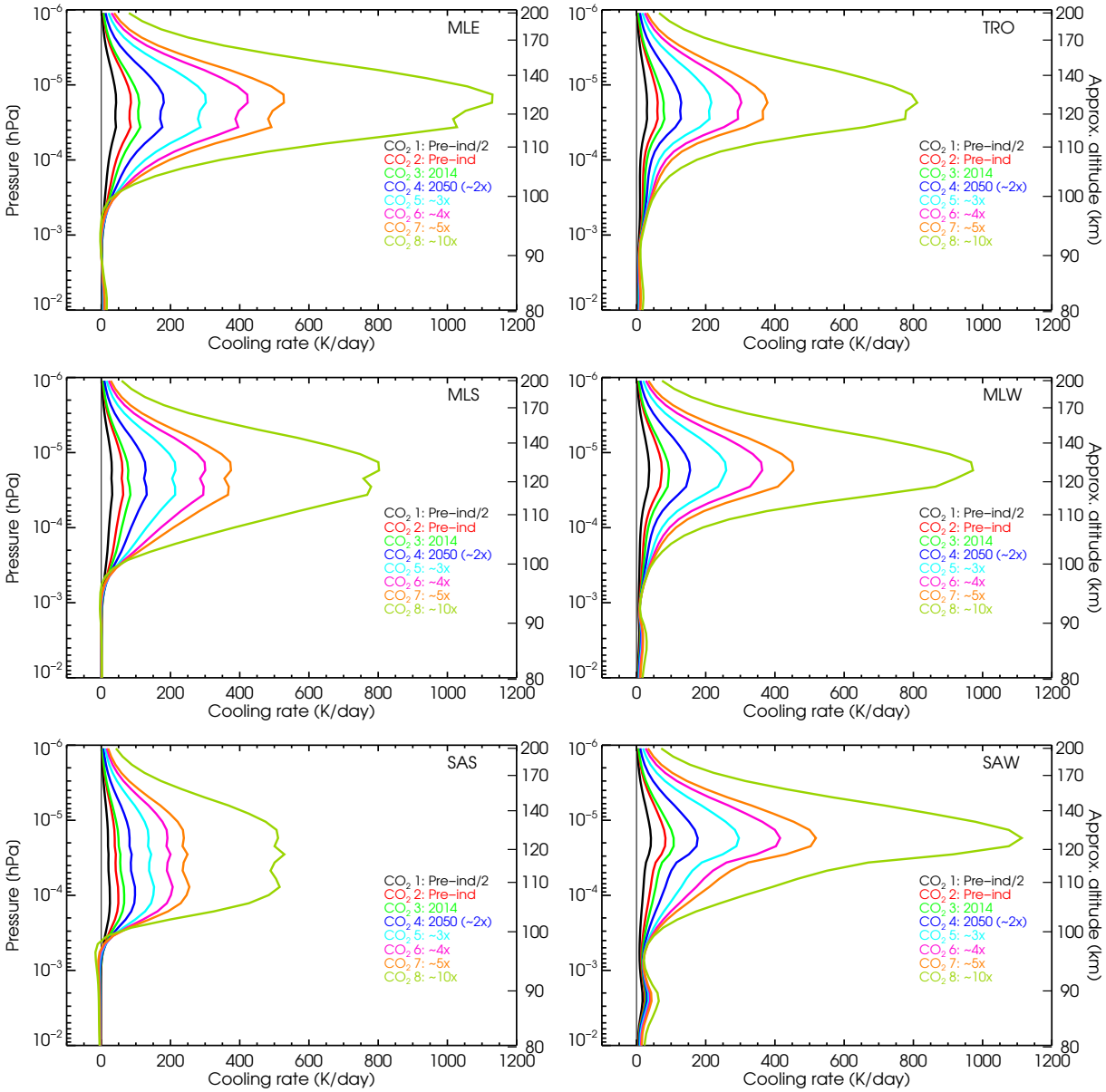

Figure S5. Non-LTE cooling rates for the reference atmospheres covering the thermosphere. Those for the lower altitudes are shown in Fig. 3 of the main paper.

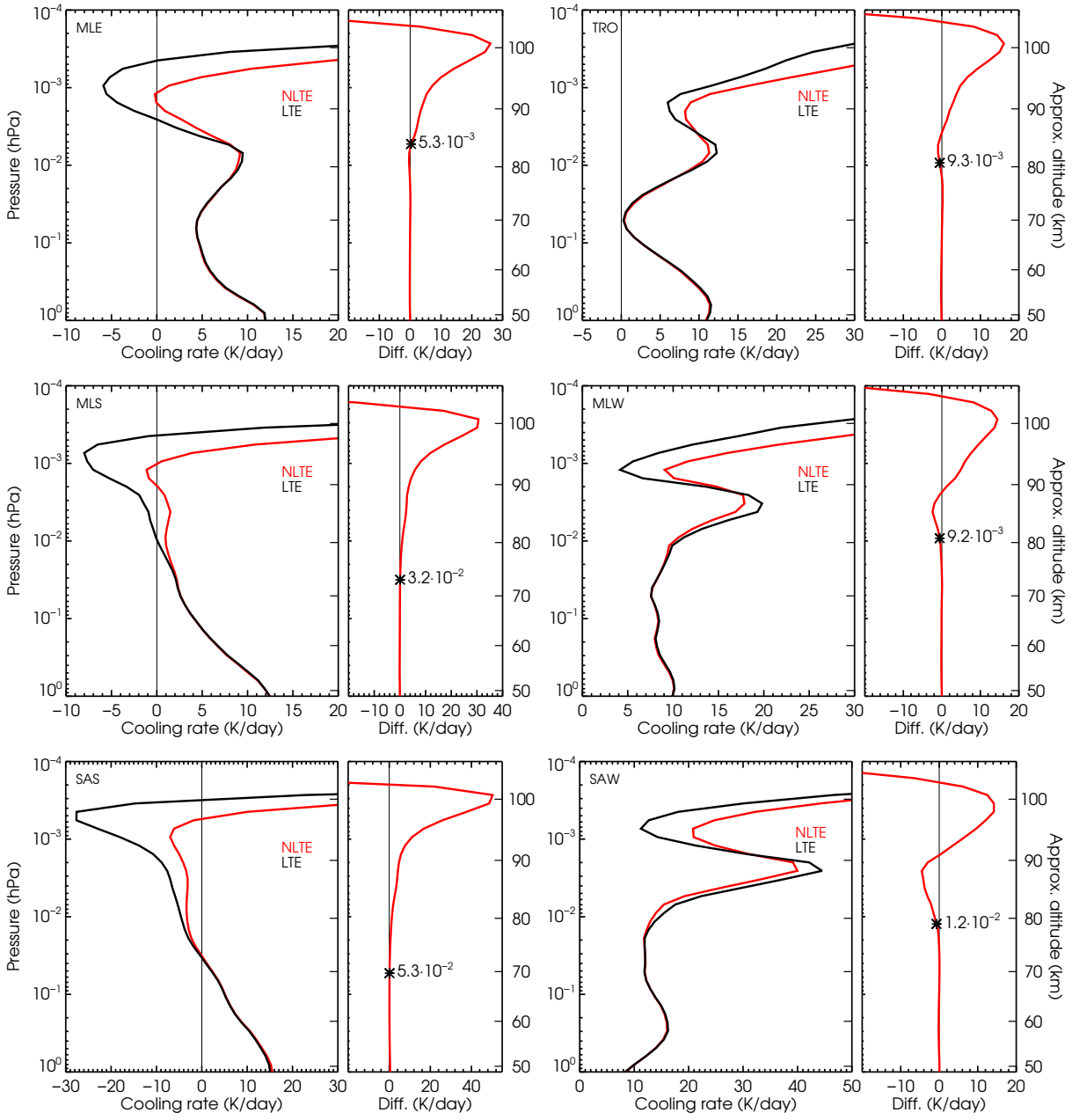

Figure S6. Non-LTE–LTE cooling rates differences for the six p–T references atmospheres (as in Fig. 5) but for the CO_2 vmr profile #6 (4× the pre-industrial values). The '*' symbol indicates the pressure level (in hPa) where the non-LTE–LTE difference reaches 5%. Note the different x-scales.

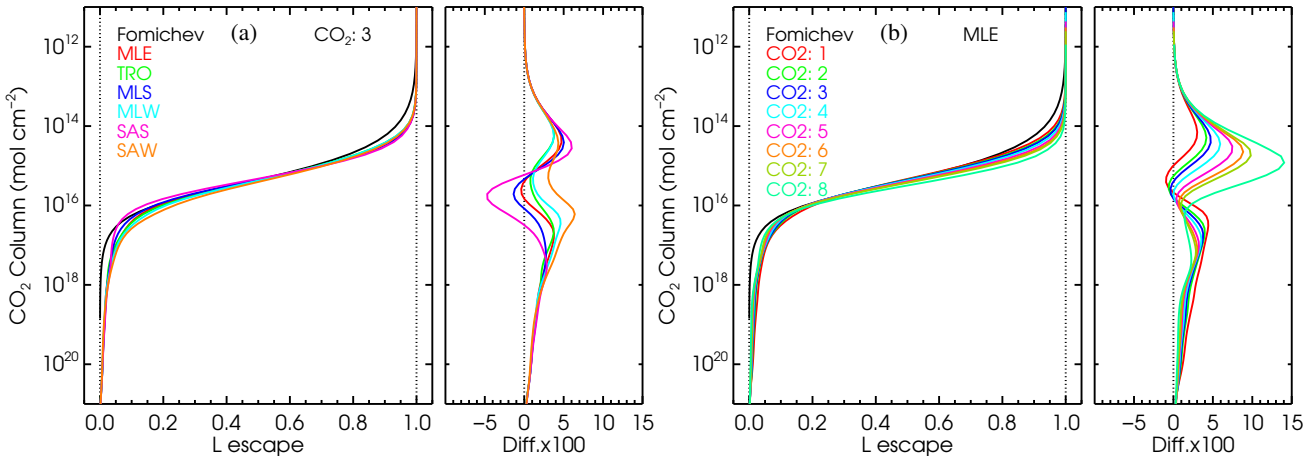

Figure S7. The escape probability function $L(u)$ represented as function of the CO_2 column at a given layer, $u(x)$, for several p-T profiles (panel a) and CO_2 vmr profiles (panel b). They have been calculated with the GRANADA code. The right panels show the differences with respect to the values used in the previous parameterization where it was used a single profile for all atmospheres. The CO_2 columns as a function of altitude are shown in Fig. S8.

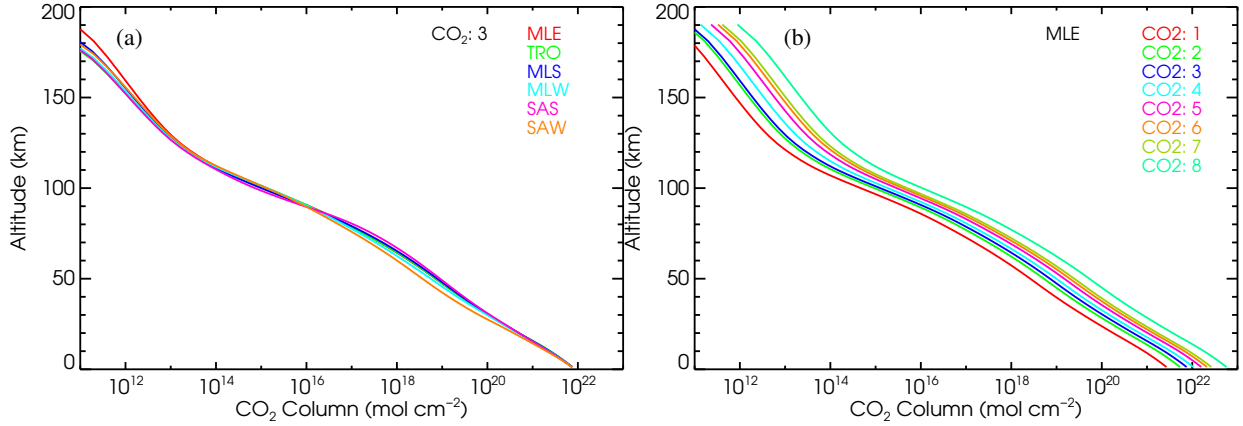

Figure S8. The CO_2 column amount u as a function of altitude z for several p-T and the current CO_2 vmr profile (#3) (panel a), and for the eight CO_2 vmr profiles considered and the mid-latitude equinox (MLE) p-T profile (panel b). They have been used in the representation of the escape probability function $L(u)$ in Fig. S7.

S1 Cooling rate differences of the current and previous parameterizations with respect to accurate cooling rates for the reference atmospheres

We show in this section a comparison of the cooling rates of the current and previous parameterizations with respect to the reference cooling rates for several CO_2 vmr profiles for the six p-T reference atmospheres. Note that similar figures for the present-day CO_2 vmr profile (#3) are shown in the main text (Fig. 8).

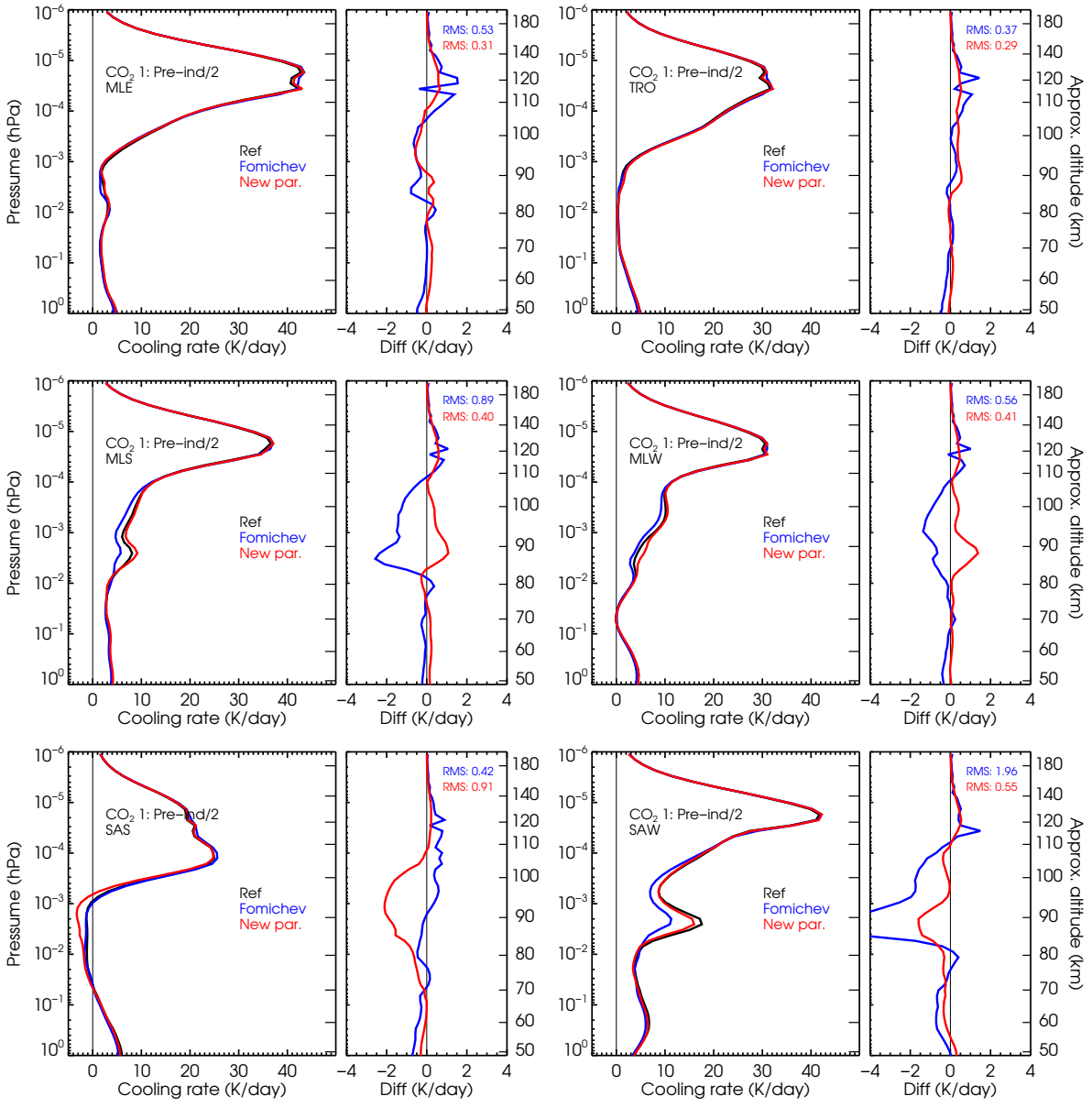

Figure S9. Comparison of the cooling rates of the current and previous parameterizations with respect to accurate cooling rates for the CO_2 vmr profile #1 (half of the preindustrial value) for the six p-T reference atmospheres.

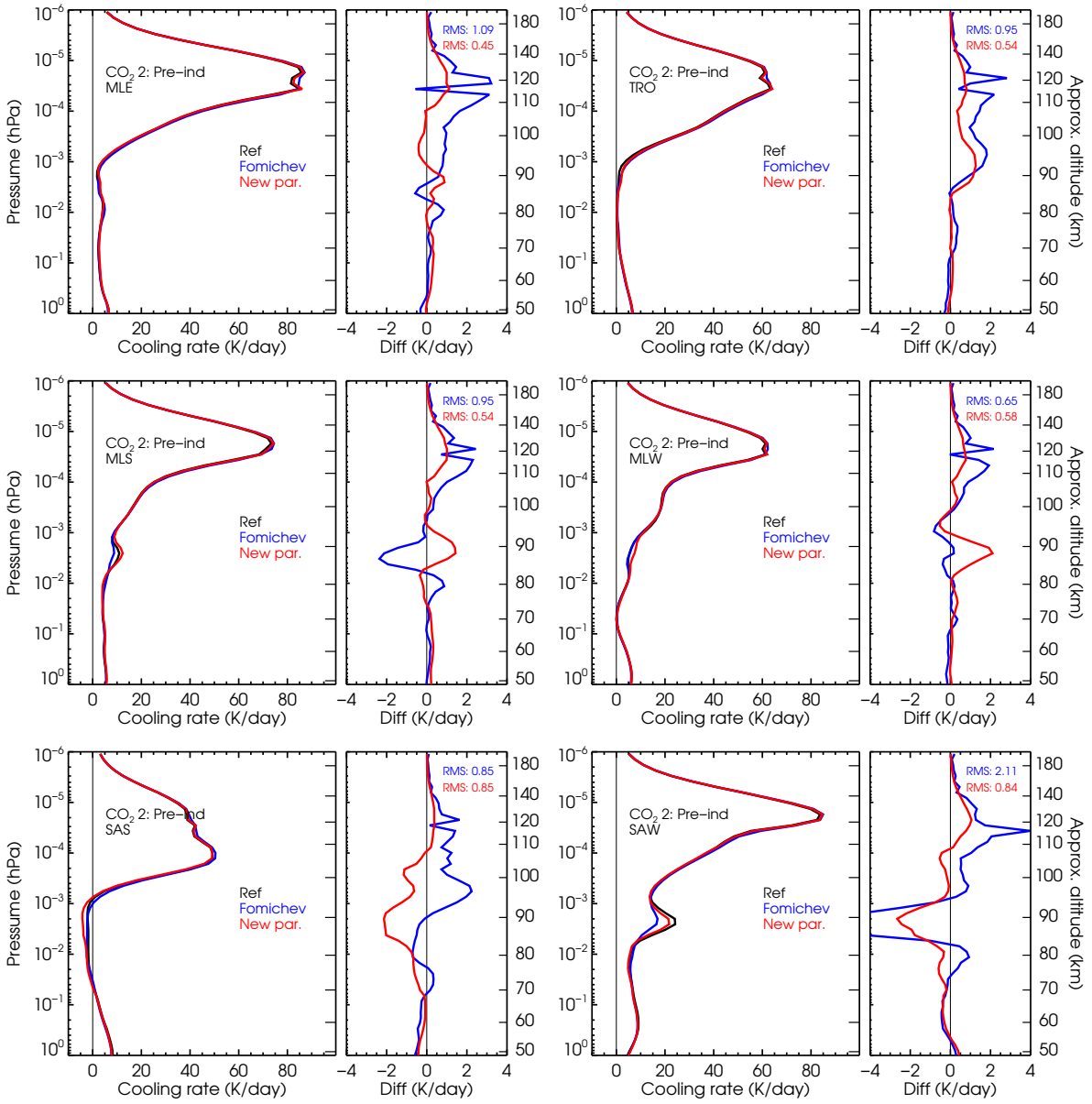

Figure S10. Comparison of the cooling rates of the current and previous parameterizations with respect to accurate cooling rates for the CO_2 vmr profile #2 (preindustrial value) for the six p-T reference atmospheres.

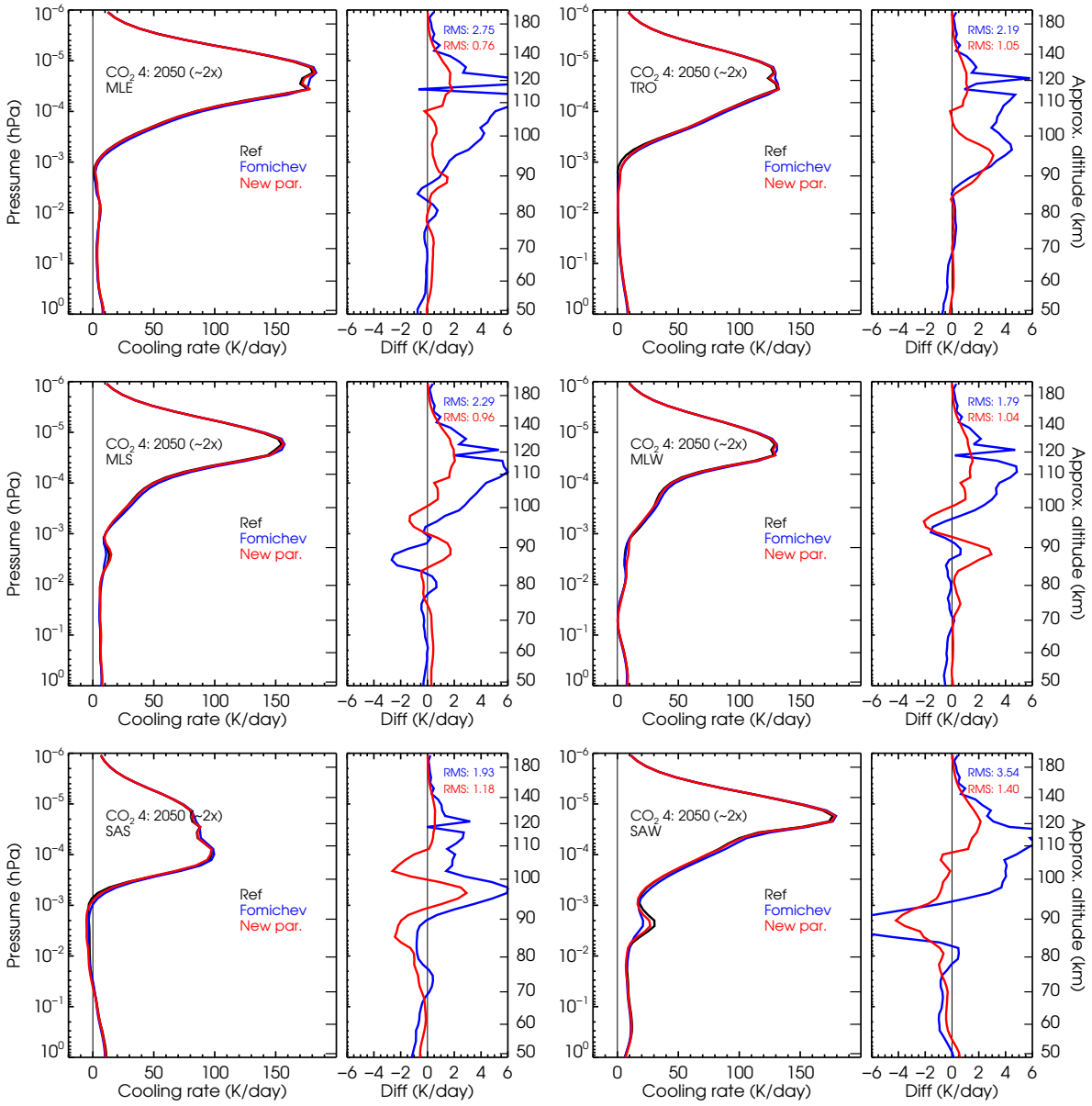

Figure S11. Comparison of the cooling rates of the current and previous parameterizations with respect to accurate cooling rates for the CO_2 vmr profile #4 ($\sim$2$\times$pre-industrial) for the six p-T reference atmospheres.

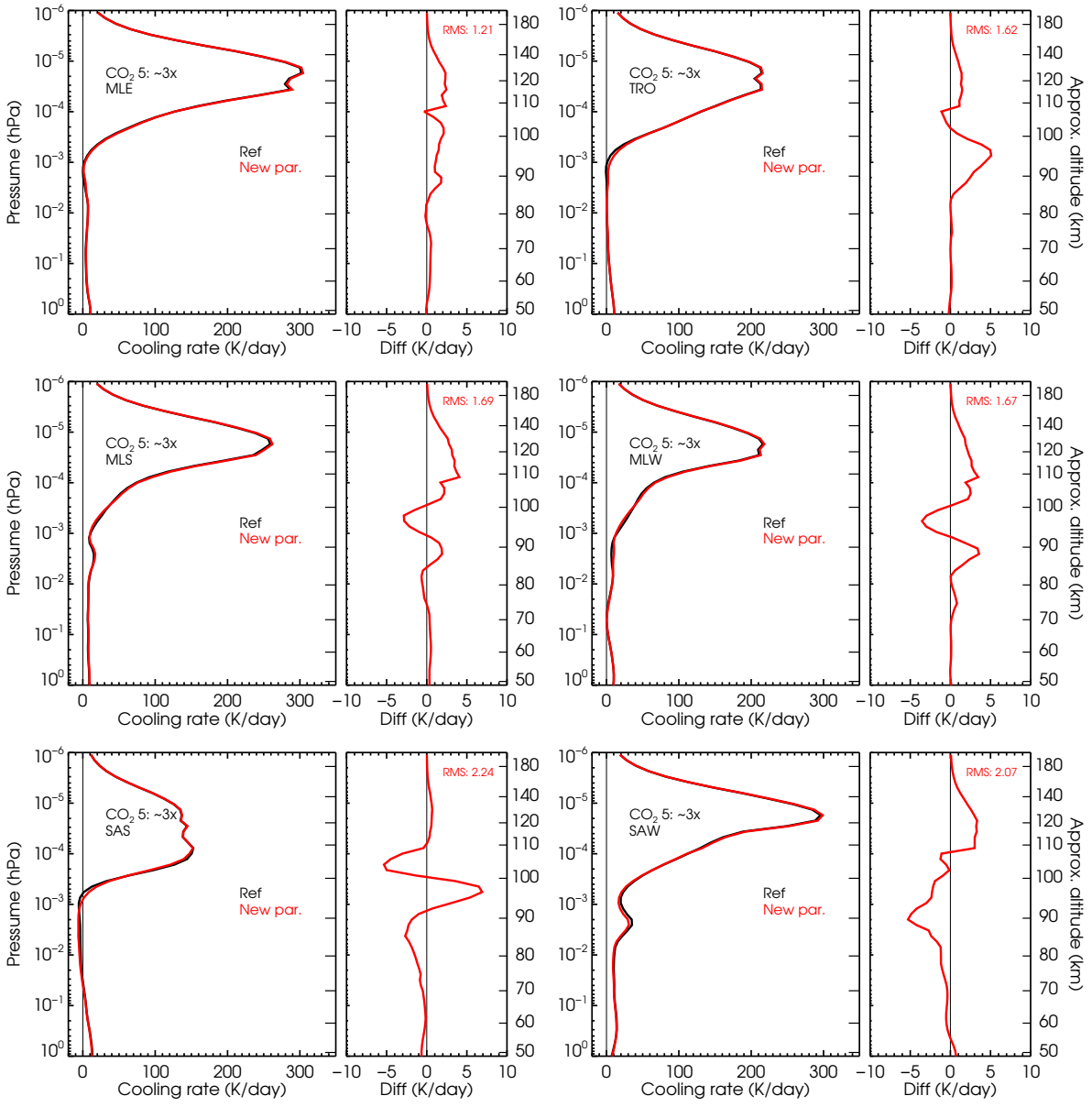

Figure S12. Comparison of the cooling rates of the current parameterization with respect to accurate cooling rates for the CO_2 vmr profile #5 ($\sim$3$\times$pre-industrial) for the six p-T reference atmospheres. The results of the previous parameterization are not shown because this CO_2 profile is beyond its applicability limits.

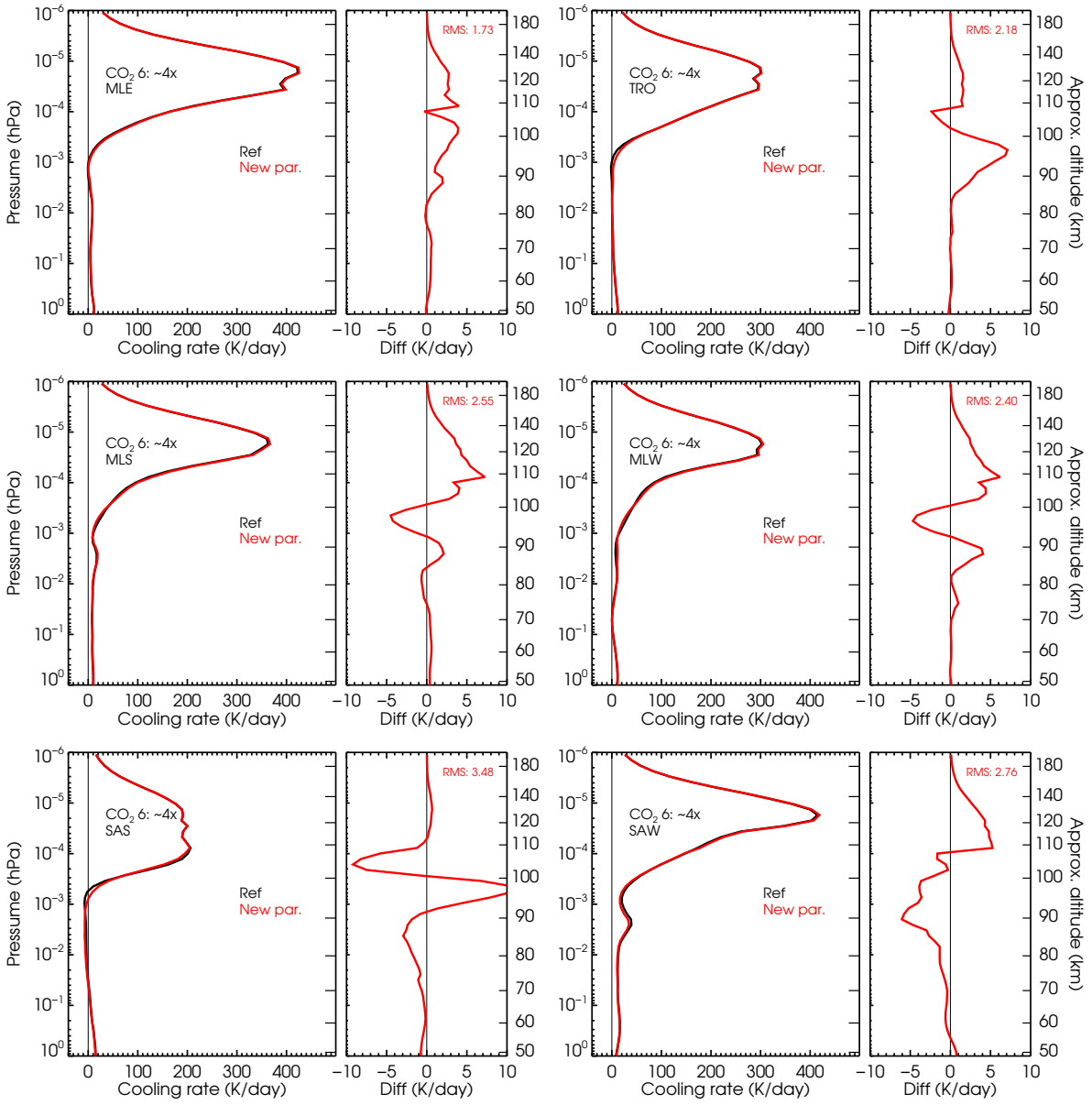

Figure S13. Comparison of the cooling rates of the current parameterization with respect to accurate cooling rates for the CO_2 vmr profile #6 ($\sim$4$\times$pre-industrial) for the six p-T reference atmospheres. The results of the previous parameterization are not shown because this CO_2 profile is beyond its applicability limits.

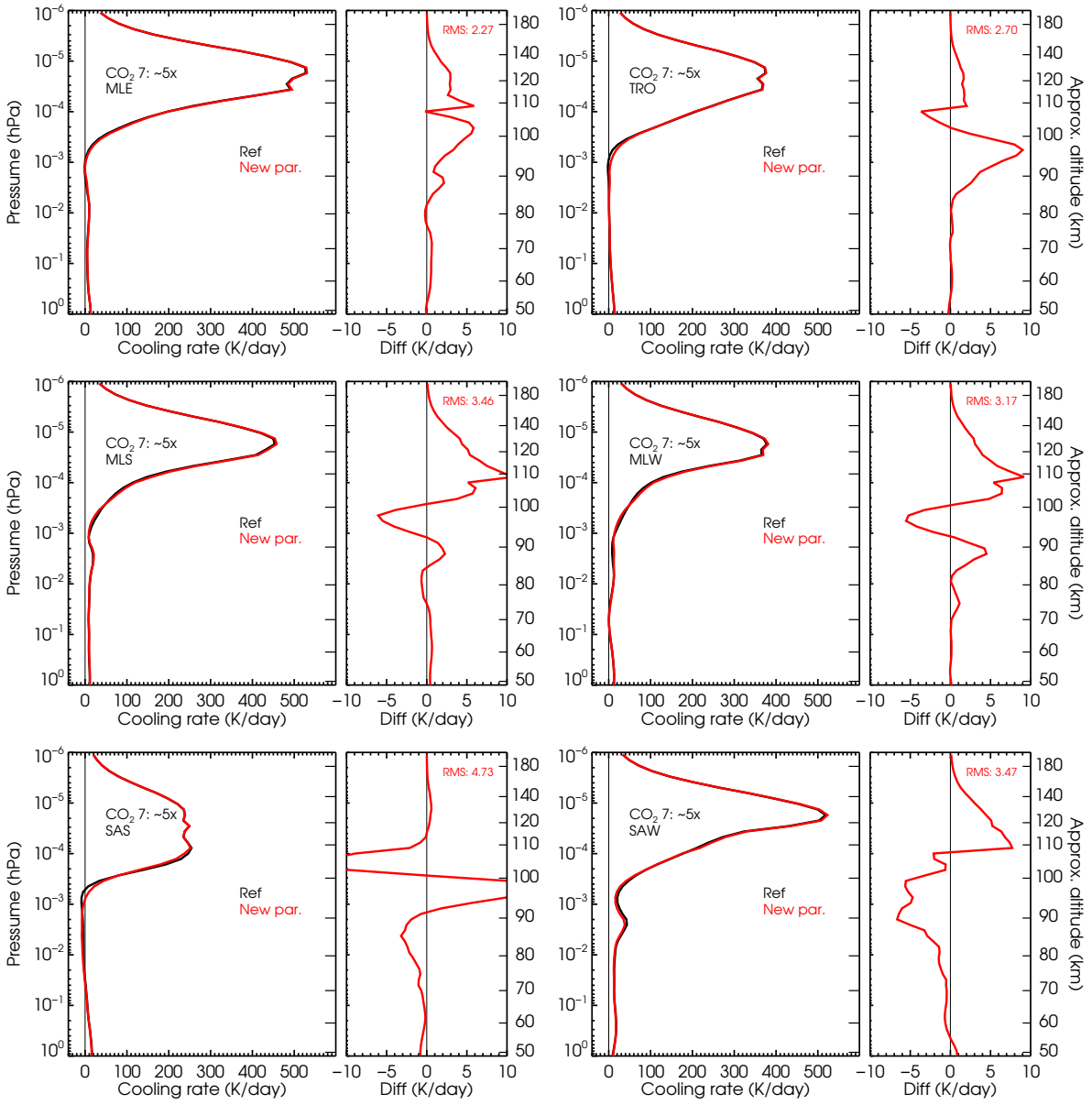

Figure S14. Comparison of the cooling rates of the current parameterization with respect to accurate cooling rates for the CO_2 vmr profile #7 ($\sim$5$\times$pre-industrial) for the six p-T reference atmospheres. The results of the previous parameterization are not shown because this CO_2 profile is beyond its applicability limits.

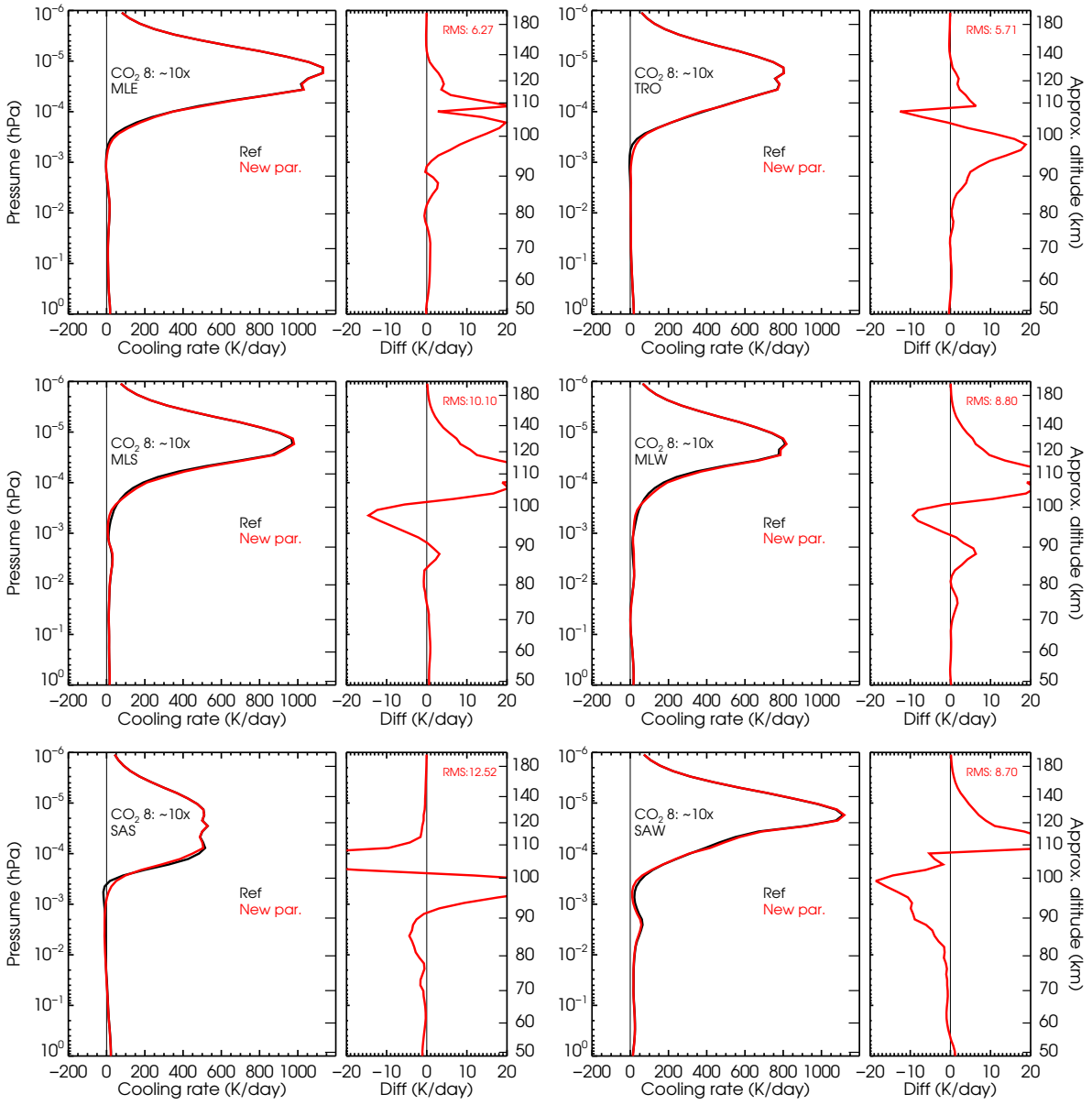

Figure S15. Comparison of the cooling rates of the current parameterization with respect to accurate cooling rates for the CO_2 vmr profile #8 ($\sim$10$\times$pre-industrial) for the six p-T reference atmospheres. The results of the previous parameterization are not shown because this CO_2 profile is beyond its applicability limits.

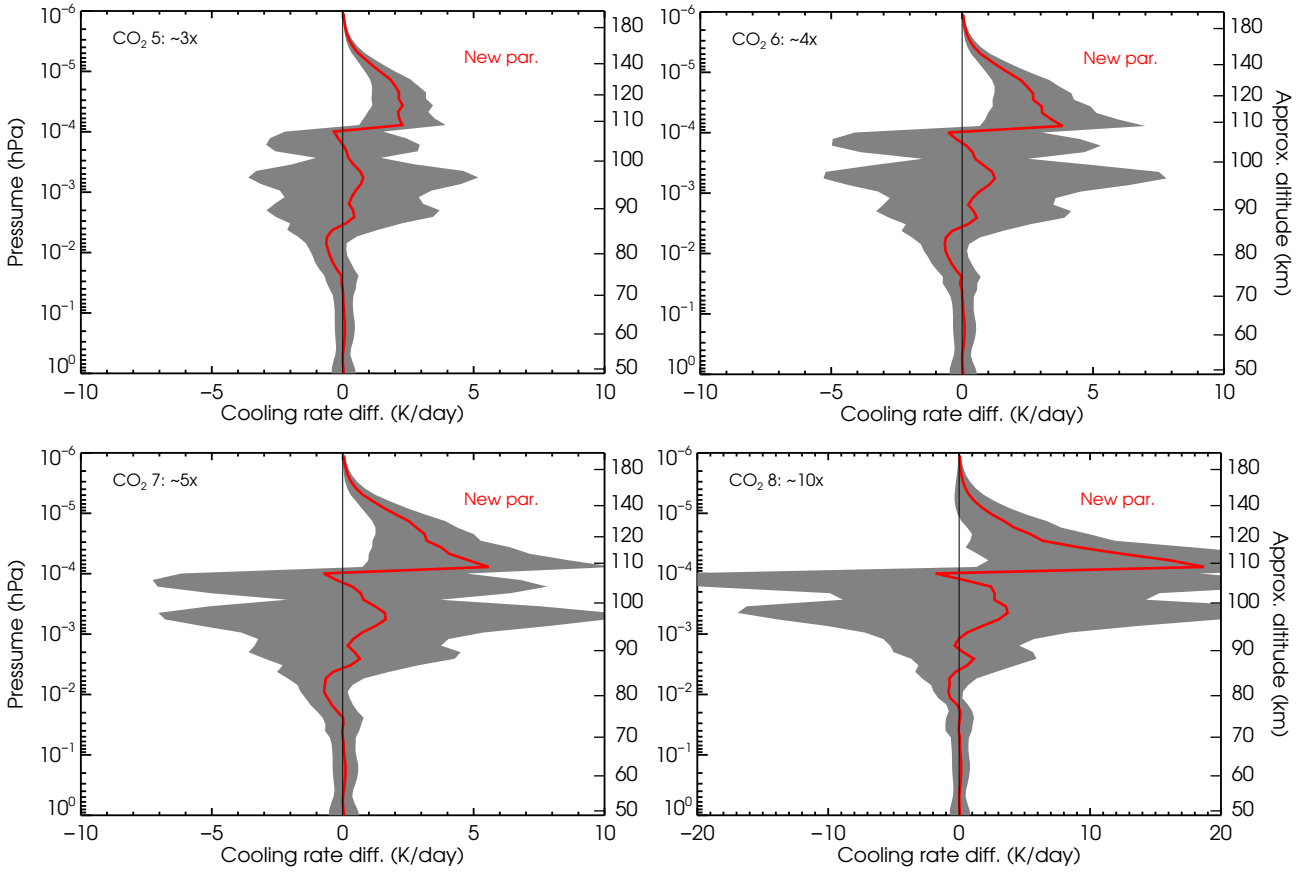

Figure S16. Mean of the cooling rates differences of the current parameterization with respect to the reference non-LTE cooling rates for the four highest CO_2 vmr profiles (#5–8) considered in this work. The shaded areas show the differences spread (standard deviation) between the six p-T atmospheres. Detailed comparisons for each $p-T$ profile are shown in Figs. S12–S15.

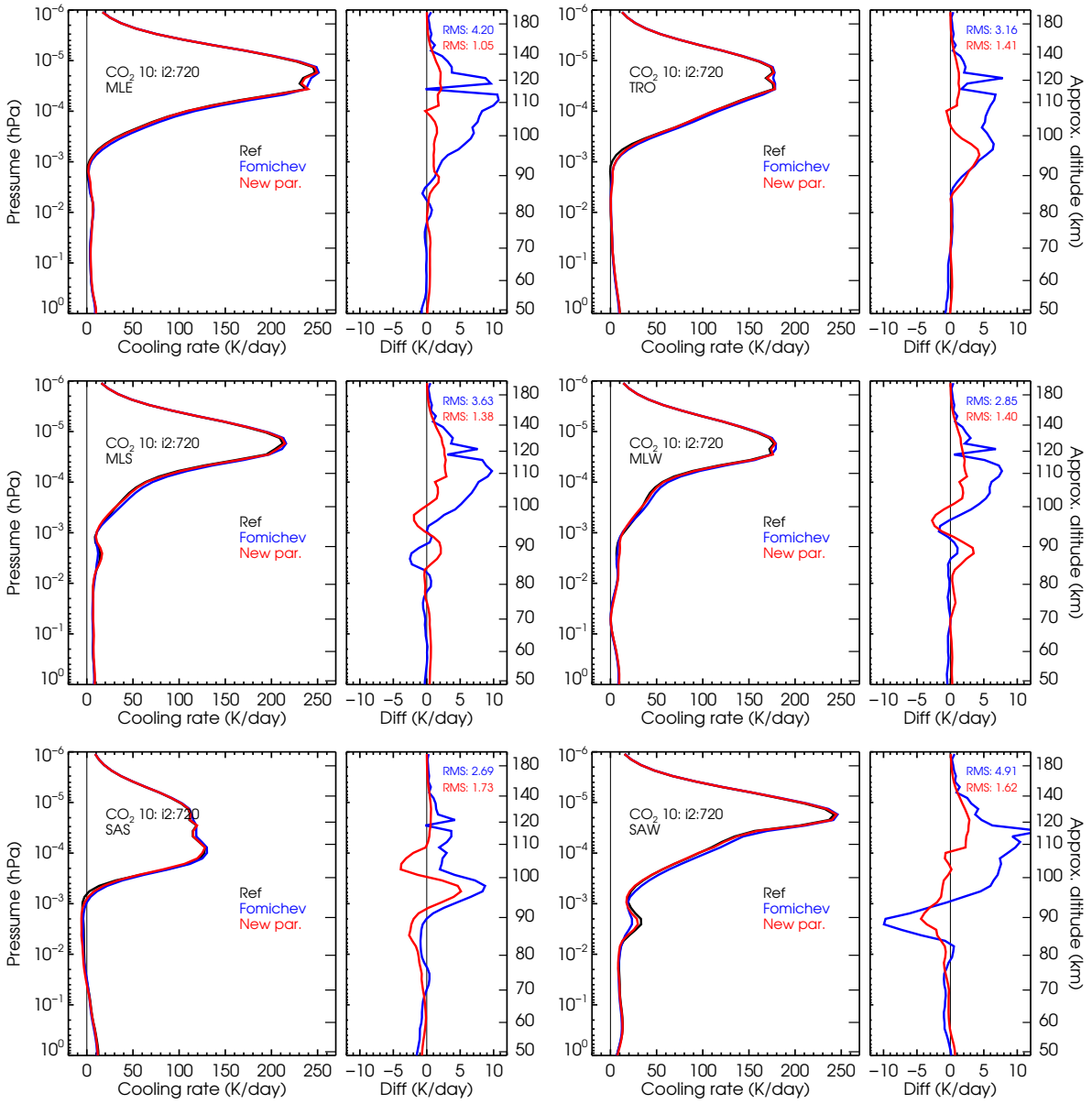

Figure S17. Comparison of the cooling rates of the current and previous parameterizations with respect to accurate cooling rates for the higher intermediate CO_2 vmr profile #10 (see Fig. 1b).

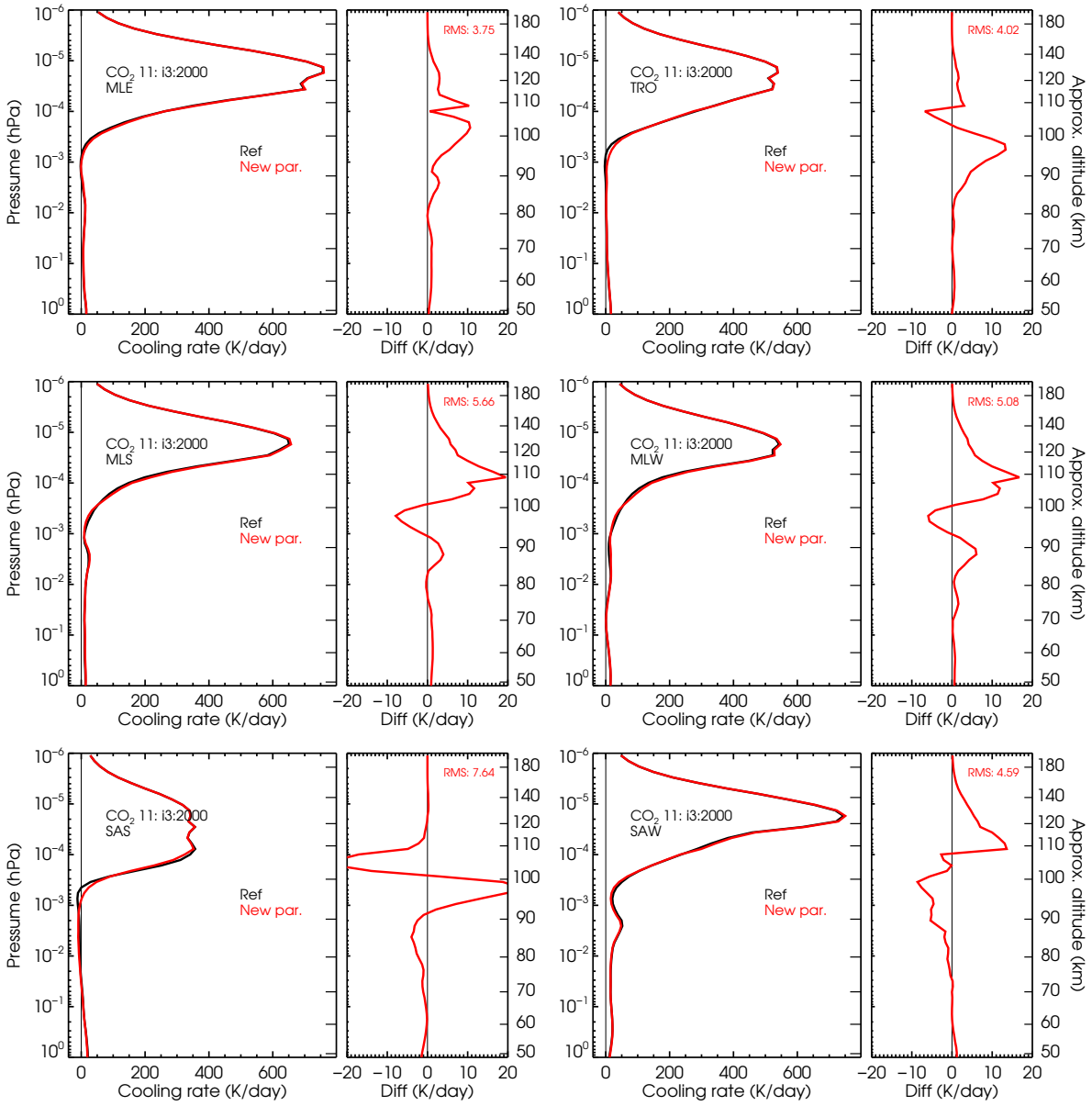

Figure S18. As Fig. S17 but for the higher intermediate CO_2 vmr profile #11 (see Fig. 1b). Note that the results of the previous parameterization are not shown as the CO_2 profile used here is beyond its applicability limits.

S2 Quantities used in the calculation of the accurate and parameterized cooling rates for the MIPAS temperatures

We show in this appendix the CO_2 vmr and $O(^3P)$ abundances used in the calculations of the accurate and parameterized cooling rates. The accurate cooling rates are also shown for reference.

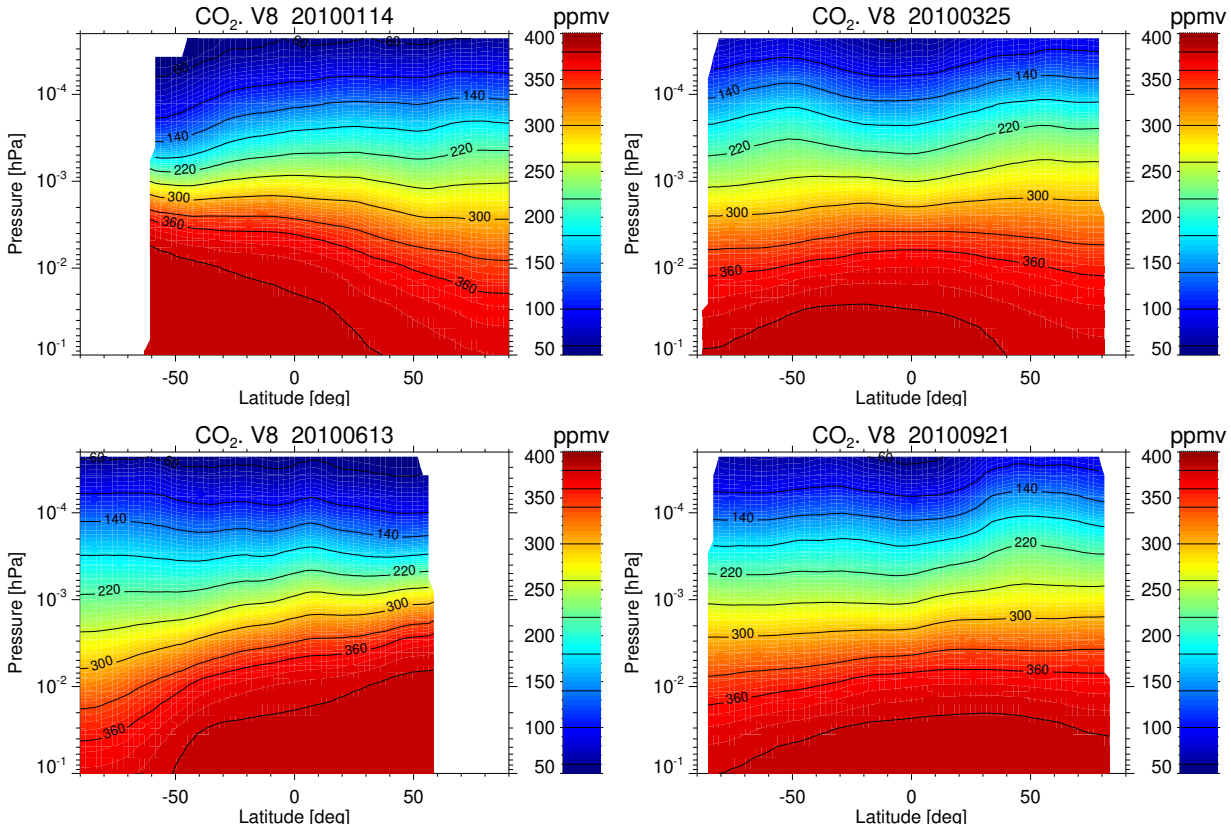

Figure S19. Zonal mean nighttime CO_2 vmrs used in the calculation of the MIPAS cooling rates.

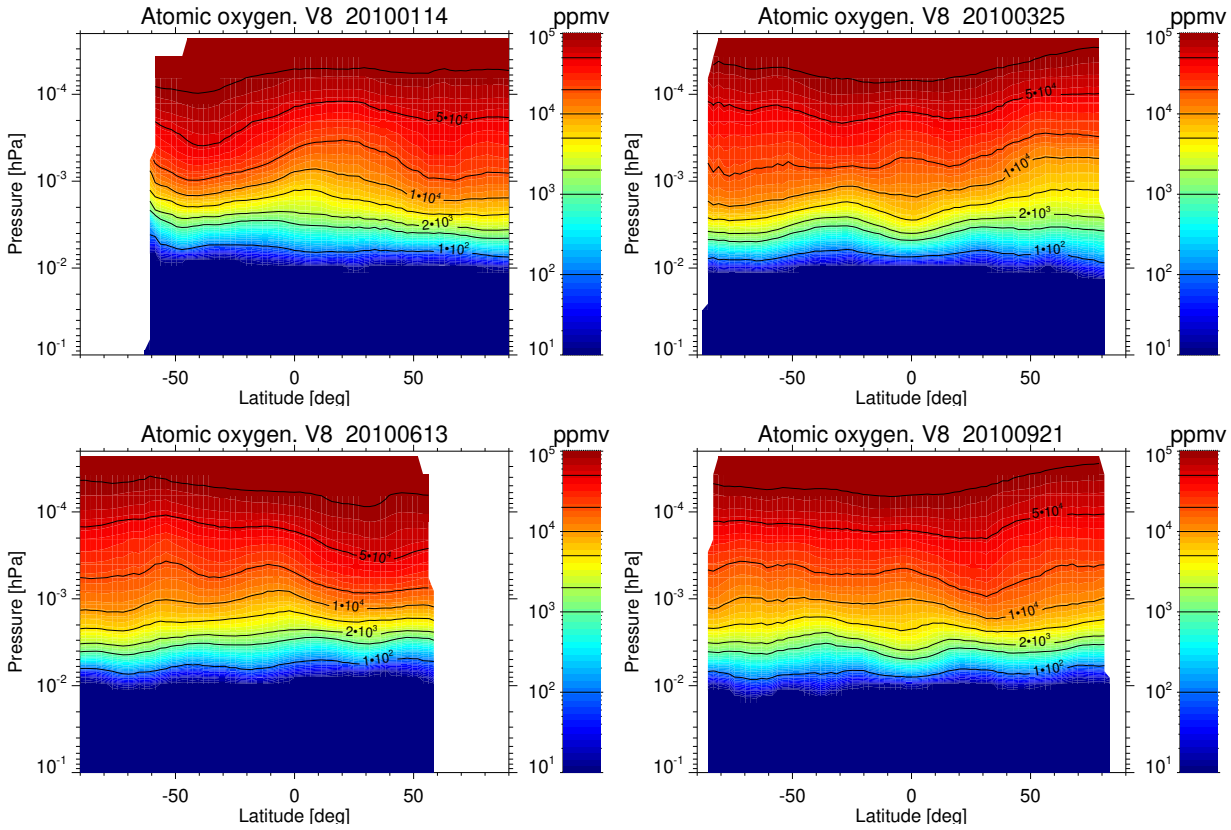

Figure S20. Zonal mean nighttime O(^3P) vmr used in the calculation of the MIPAS cooling rates.

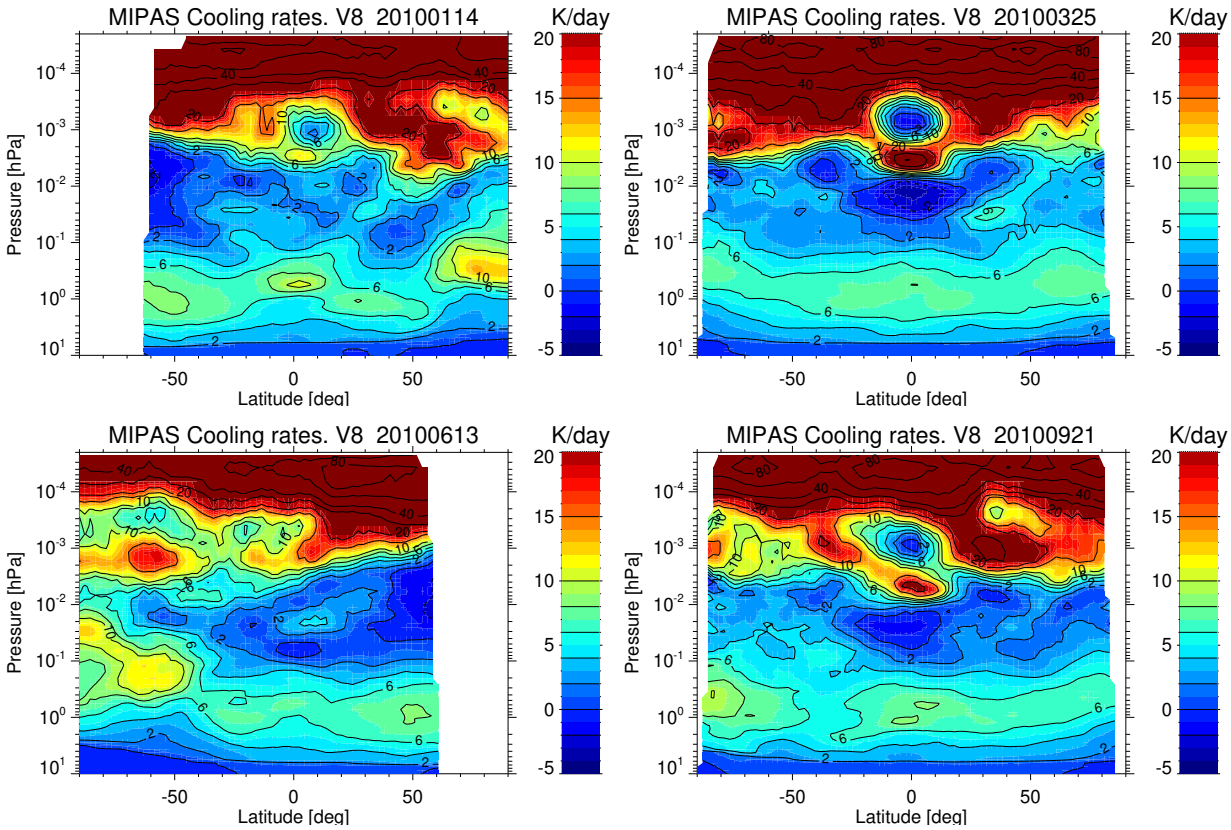

Figure S21. Zonal mean accurate cooling rates obtained for the MIPAS nighttime temperatures considered in this work.

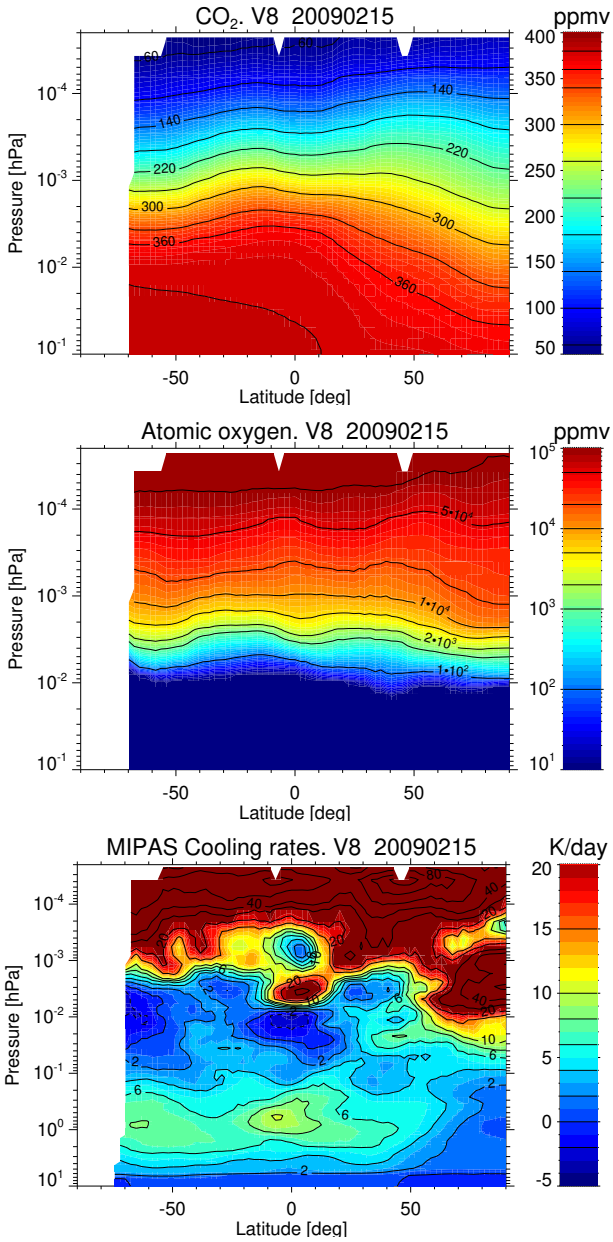

Figure S22. Zonal mean of the CO_2 vmr (top), O(^3P) abundance (middle) and the LBL accurate cooling rates (bottom) for the elevated stratopause conditions (15 February 2009).

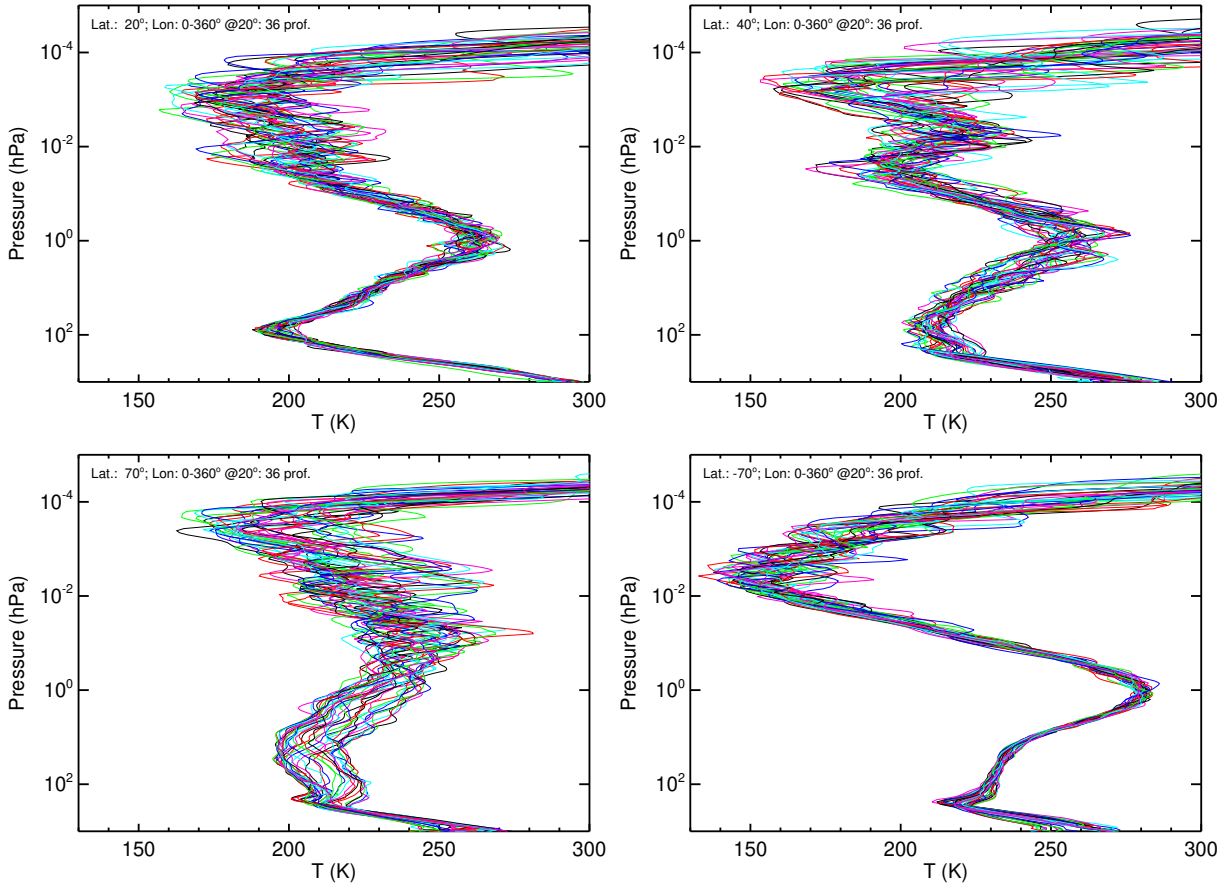

Figure S23. Pressure-temperature profiles from WACCM-X used to test the parameterization. The panels are for four latitudes, 20°N, 60°N, 70°N and 70°S for January conditions. In each panel, 36 profiles are plotted corresponding to longitudes from 0° to 360° every 10°.

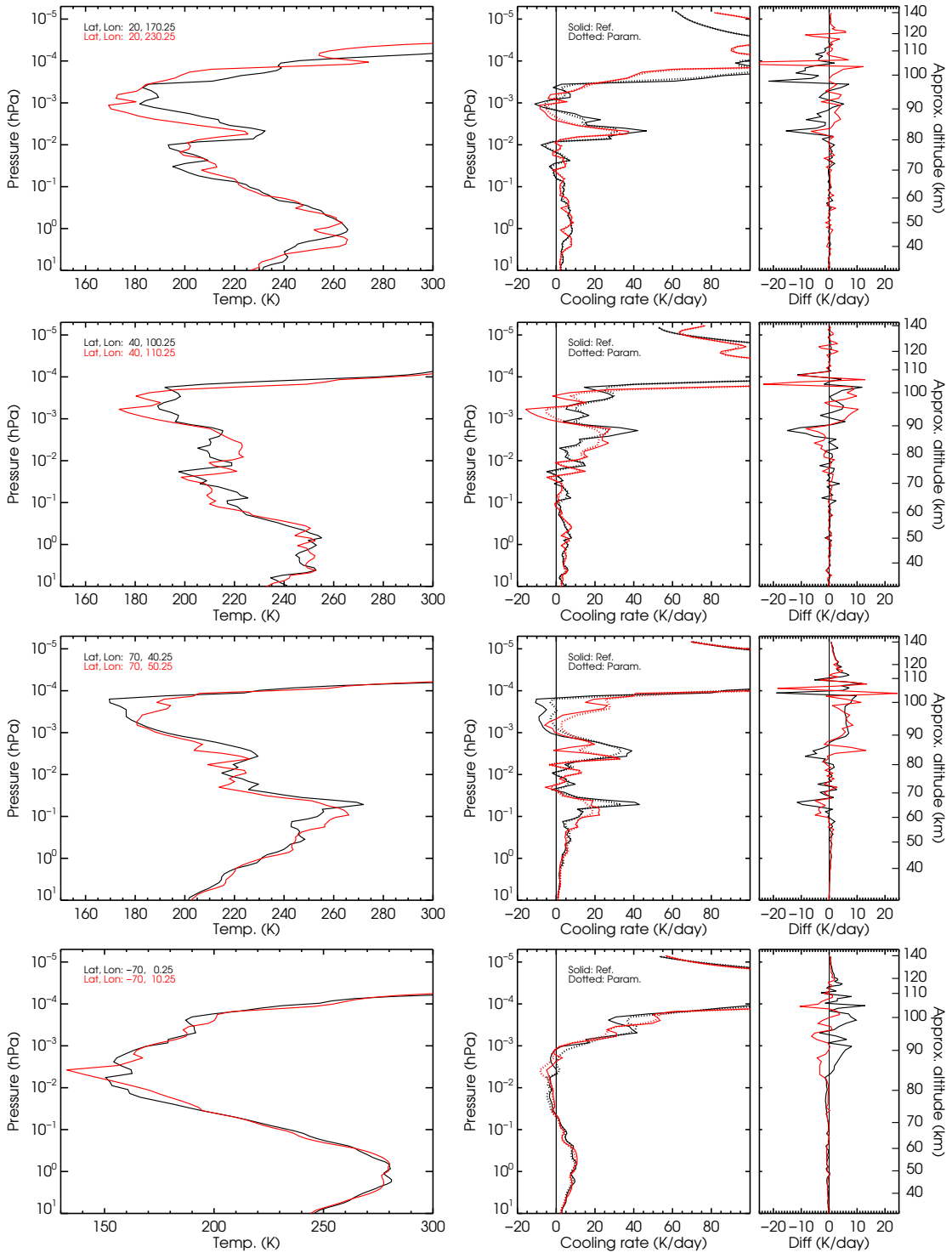

Figure S24. Comparison of cooling rates of the parameterization and reference calculations for some high-resolution WACCM-X temperature profiles. As Fig. 16 but for p-T profiles for different longitudes.

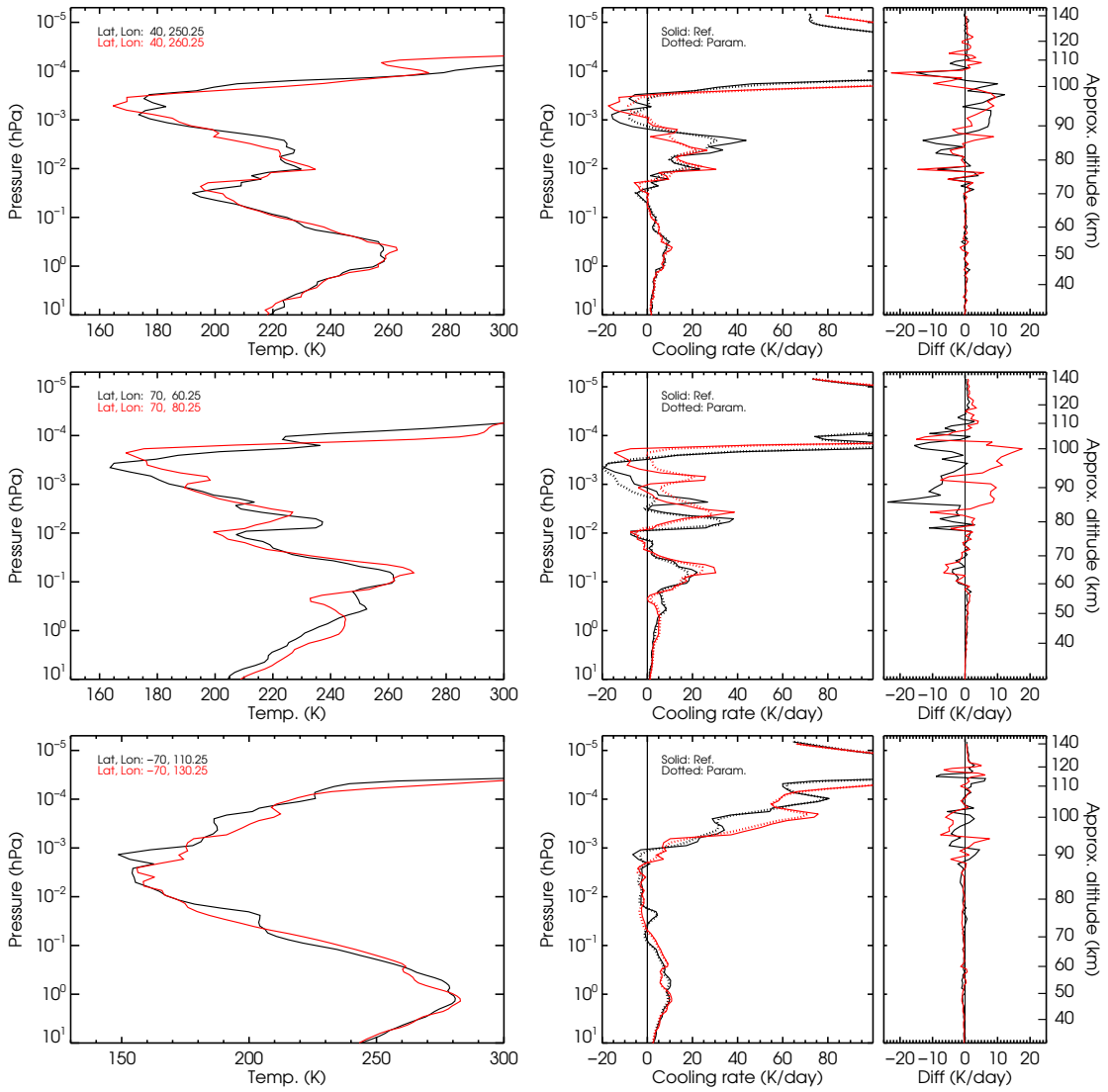

Figure S25. Comparison of cooling rates of the parameterization and reference calculations for high-resolution WACCM-X temperature profiles. As Fig. S24 but for p-T profiles for different longitudes.

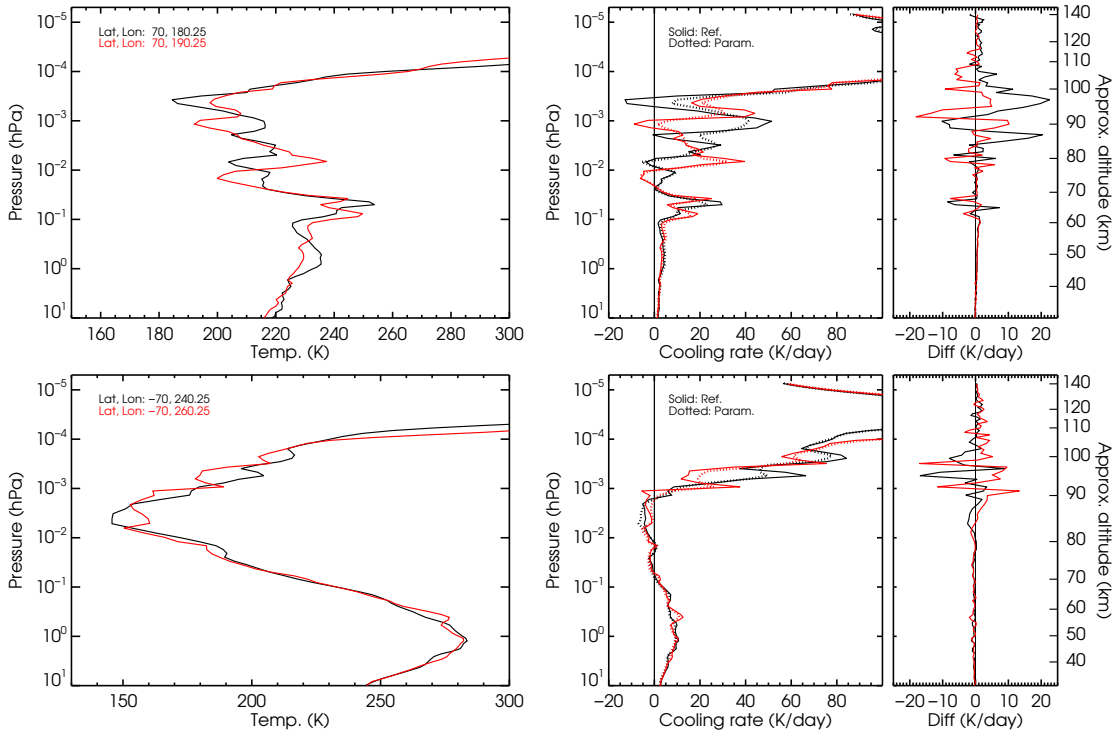

Figure S26. Comparison of cooling rates of the parameterization and reference calculations for high-resolution WACCM-X model temperature profiles. As Figs. S24 but for p-T profiles for different longitudes.